



ELSEVIER

Physica B 219&220 (1996) 80–82

PHYSICA B

Lattice thermal conductivity of Nb-based alloy superconductors and phonon scattering by electrons

M. Ikebe^{a,*}, T. Naito^a, H. Fujishiro^a, K. Noto^a, N. Kobayashi^b, K. Mori^c

^aFaculty of Engineering, Iwate University, 4-3-5, Ueda, Morioka 020, Japan

^bInstitute for Materials Research, Tohoku University, Sendai 980, Japan

^cFaculty of Engineering, Toyama University, Toyama 930, Japan

Abstract

Quantitative analyses for the thermal conductivity in the superconducting state of $\text{Nb}_{1-x}\text{Ta}_x$ and $\text{Nb}_{1-x}\text{Mo}_x$ alloy systems were performed applying the revised Bardeen, Rickayzen and Tewordt theory. The correlation between T_c and the strength of the electron–phonon interaction was clearly demonstrated. Addition of Mo to Nb was found to reduce promptly the electron–phonon interaction, resulting in the reduction of T_c .

1. Introduction

One useful method to evaluate phonon–electron interaction in superconductors is to analyze the temperature variation of the thermal conductivity in the superconducting state. This method is especially suitable for alloy superconductors, in which the electron transport is limited by impurity scattering and a considerable part of the heat flux is due to phonons. In such a case, the classical theory of Bardeen, Rickayzen and Tewordt (BRT) [1] is known to explain well the temperature variation of the thermal conductivity in the superconducting state, i.e., the quenching of the electron component due to the formation of the Cooper pairs and the enhancement of the phonon component due to the quenching of phonon scattering by electrons. Recently, Tewordt and Wölkhäusen (TW) [2] generalized the BRT theory by taking account of other phonon scattering centers as well. We apply the TW procedure to typical classical alloy systems, $\text{Nb}_{1-x}\text{Ta}_x$ [3, 4] and $\text{Nb}_{1-x}\text{Mo}_x$ [5] and clarify

how the electron–phonon interaction manifests itself in the thermal conductivity below T_c .

2. Experimental

Nb–Ta and Nb–Mo alloys were prepared by melting the constituent metals (with 99.9% purity) in an Ar arc furnace about ten times to promote homogeneity. The resultant alloy buttons were finally remelted in an electron beam furnace under a vacuum of 10^{-6} mmHg. The thermal conductivity was measured by a usual continuous heat flow method in He^4 (1.2–4.2 K) and He^3 (0.5–1.2 K) cryostats. Carbon resistors were used as thermometers. In order to measure the normal state conductivity, magnetic fields were applied perpendicular to the heat flow direction.

3. Results and discussion

Fig. 1 shows, as a typical example, the thermal conductivity of $\text{Nb}_{80}\text{Ta}_{20}$ as a function of the temperature

* Corresponding author.

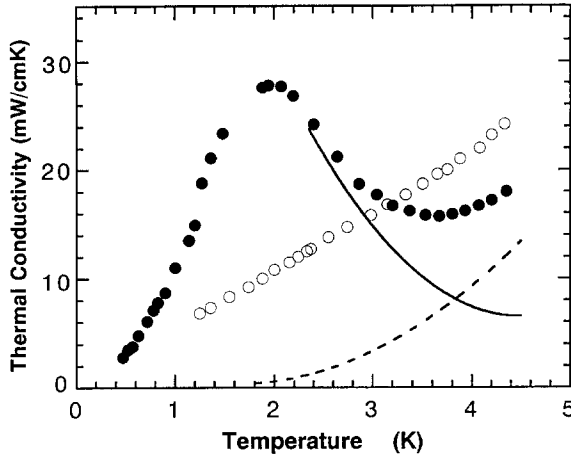


Fig. 1. The thermal conductivity of $Nb_{80}Ta_{20}$ versus T [3]. Solid and open circles denote the data in the superconducting and normal states, respectively. Dashed and solid curves indicate the electron and phonon component in the superconducting state.

for both the superconducting and normal states. The electron component of the heat flux in the superconducting state κ_{es} relative to that in the normal state κ_{en} was calculated by the following BRT formula:

$$\kappa_{es}/\kappa_{en} = \{2F(-y) + 2y \ln(1 + I^{-y}) + y^2(1 + I^y)^{-1}\}/2F(0), \quad (1)$$

$$F(y) = \int_0^x \frac{z}{(1 + e^{z+y})} dz \quad \text{and} \quad y = \frac{\Delta(T)}{k_B T}. \quad (2)$$

The energy gap $\Delta(T)$ was assumed to obey the standard BCS theory. By subtracting the electronic contribution following these equations, the obtained phonon thermal conductivity in the superconducting state κ_{gs} is given in Fig. 2 for $Nb_{1-x}Ta_x$ and in Fig. 3, for $Nb_{1-x}Mo_x$, respectively. Then, κ_{gs} was analyzed using the following TW formulation:

$$\kappa_{gs} = \frac{k_B}{2\pi^2 v} \left(\frac{k_B}{\hbar}\right)^3 T^3 \int_0^{\Theta_D/T} \frac{x^4 e^x}{(e^x - 1)} \tau_{phs} dx, \quad (3)$$

where Θ_D is the Debye temperature, v the sound velocity and $x (= \hbar\omega/k_B T)$ is the reduced phonon frequency. The phonon relaxation time in the superconducting state τ_{phs} is expressed as

$$\tau_{phs}^{-1} = \tau_b^{-1} + \tau_d^{-1} + \tau_p^{-1} + \tau_c^{-1} = \tau_b^{-1} + DTx + pT^4 x^4 + EgTx. \quad (4)$$

Here, τ_b is the phonon relaxation time due to boundaries and D , p , and E refer to the strength of the phonon scattering due to dislocations, point defects and elec-

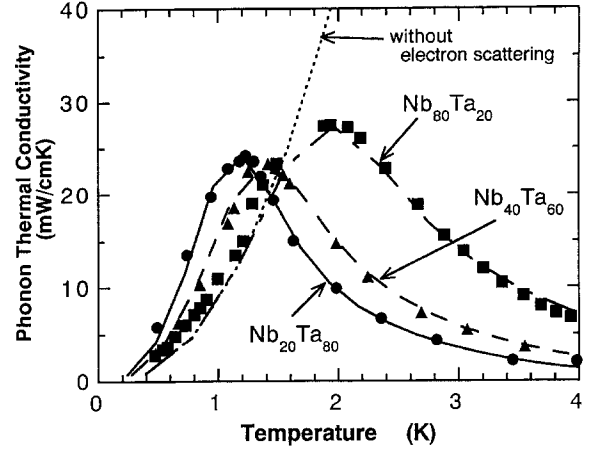


Fig. 2. Phonon thermal conductivity of $Nb_{1-x}Ta_x$ in the superconducting state and TW fitting lines.

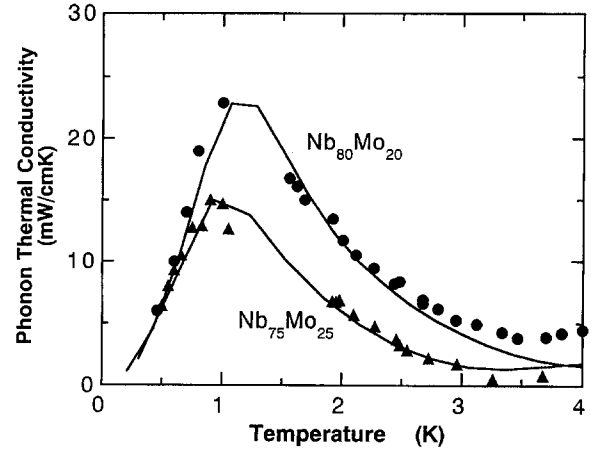


Fig. 3. Phonon thermal conductivity of $Nb_{1-x}Mo_x$ in the superconducting state and TW fitting lines.

trons, respectively. The phonon scattering ratio g by electrons in the superconducting and normal state was also given by BRT. In this analysis, p was assumed to be zero because the point defect scattering is not effective in such a low-temperature region below 4 K. The best fitting curves are shown in Figs. 2 and 3. The parameters used and determined in the fitting are summarized in Table 1. In this table, we notice that the values of E , the strength of the phonon scattering by electrons (= quasiparticles in the superconducting state), is larger for samples with higher T_c . Comparing $Nb_{80}Mo_{20}$ with $Nb_{80}Ta_{20}$, we also notice much reduced E value of $Nb_{80}Mo_{20}$ accompanied with the remarkable reduction of T_c . In order to show the temperature dependence of

Table 1

Characteristic parameters of the $\text{Nb}_{1-x}\text{Ta}_x$ and $\text{Nb}_{1-x}\text{Mo}_x$ alloys. For comparison, those of $\text{YBa}_2\text{Cu}_3\text{O}_7$ (90 K phase) and $\text{YBa}_2\text{Cu}_3\text{O}_{7-\delta}$ (60 K phase) were also presented [7]

Parameters	$\text{Nb}_{80}\text{Ta}_{20}$	$\text{Nb}_{40}\text{Ta}_{60}$	$\text{Nb}_{20}\text{Ta}_{80}$	$\text{Nb}_{80}\text{Mo}_{20}$	$\text{Nb}_{75}\text{Mo}_{25}$	$\text{YBa}_2\text{Cu}_3\text{O}_7$ (90 K phase)	$\text{YBa}_2\text{Cu}_3\text{O}_{7-\delta}$ (60 K phase)
τ_b^{-1} (s^{-1})	2.8×10^7	7.9×10^6	5.1×10^6	7.6×10^6	2.3×10^6	4.8×10^8	6.1×10^8
E ($\text{K}^{-1} \text{s}^{-1}$)	1.1×10^{10}	4.3×10^9	3.2×10^9	2.6×10^9	2.0×10^9	2.6×10^9	2.0×10^9
D ($\text{K}^{-1} \text{s}^{-1}$)	1.8×10^7	8.6×10^6	5.3×10^6	8.8×10^6	1.0×10^7	0	0
p ($\text{K}^{-4} \text{s}^{-1}$)	0	0	0	0	0	1.1×10^3	6.2×10^2
s ($\text{K}^{-2} \text{s}^{-1}$) ^a	0	0	0	0	0	1.0×10^7	8.0×10^6
Θ_D (K)	250	250	250	264 [6]	266 [6]	300	350
T_c (K)	7.85	5.52	4.82	4.28	3.41	92	62
v (m/s)	4238	3794	3572	4912	5025	3330	3530

^a s is the strength of the phonon scattering due to sheet-like faults ($\tau_s^{-1} = sT^2x^2$).

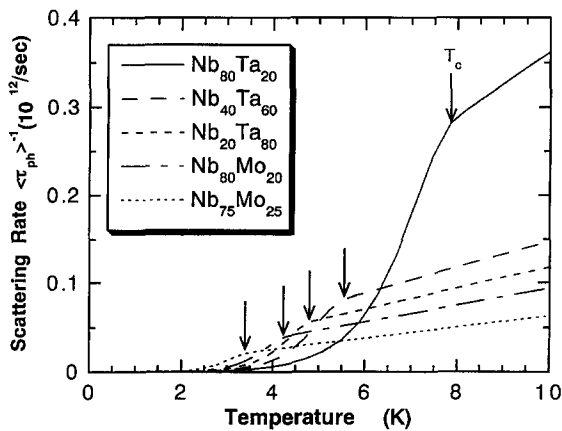


Fig. 4. Calculated average phonon scattering rate $\langle \tau_{ph} \rangle^{-1}$ versus T . In this figure, $\langle \tau_{ph} \rangle^{-1}$ can be regarded as entirely due to electron scattering.

the phonon scattering more clearly, the calculated phonon scattering rate $\langle \tau_{ph} \rangle^{-1}$ versus T is plotted in Fig. 4. The calculation of $\langle \tau_{ph} \rangle$ was performed as an average on the Debye phonon spectrum using the parameters in Table 1. On the scale of the ordinate in Fig. 4, $\langle \tau_{ph} \rangle^{-1}$ can be regarded as entirely due to electron scattering ($\langle \tau_{ph} \rangle \cong \langle \tau_{ph}^e \rangle$). At He^3 temperatures (0.5–1.2 K) where electron scattering is completely quen-

ched, both the dislocation scattering and boundary scattering are effective on the comparative intensity.

In our previous paper [7], the E values of the oxide superconductors $\text{YBa}_2\text{Cu}_3\text{O}_7$ (90 K phase) and $\text{YBa}_2\text{Cu}_3\text{O}_{7-\delta}$ (60 K phase) were estimated following the same procedure as the present analyses. The E values of YBCO were about 2×10^9 ($\text{K}^{-1} \text{s}^{-1}$) and these values are rather comparable with the present alloy systems. In view of the small carrier concentration in the oxide system, the electron–phonon interaction is unexpectedly strong and cannot be neglected, at least, in Yttrium-based oxide superconductors.

References

- [1] J. Bardeen, G. Rickayzen and L. Tewordt, Phys. Rev. 113 (1959) 982.
- [2] L. Tewordt and T. Wölkhausen, Solid State Commun. 70 (1989) 839.
- [3] N. Kobayashi, K. Noto, M. Ikebe and Y. Muto, J. Low Temp. Phys. 17 (1974) 575.
- [4] M. Ikebe, N. Kobayashi and Y. Muto, J. Phys. Soc. Japan 37 (1974) 278.
- [5] M. Ikebe, N. Kobayashi and Y. Muto, Phys. Lett. 47 A (1974) 227.
- [6] K. Mori, unpublished.
- [7] H. Fujishiro, M. Ikebe, T. Naito and K. Noto, Physica C 235–240 (1994) 825.